Atmospheric Environment 182 (2018) 128–137

Contents lists available at ScienceDirect

Atmospheric Environment

journal homepage: www.elsevier.com/locate/atmosenv

Sources of variance in BC mass measurements from a small marine engine: Influence of the instruments, fuels and loads

Yu Jiang[a,b], Jiacheng Yang[a,b], Stéphanie Gagné[c], Tak W. Chan[d,i], Kevin Thomson[c], Emmanuel Fofie[a,b,j], Robert A. Cary[f], Dan Rutherford[g], Bryan Comer[g], Jacob Swanson[h], Yue Lin[a,e], Paul Van Rooy[a,b], Akua Asa-Awuku[a,b,j], Heejung Jung[a,e], Kelley Barsanti[a,b], Georgios Karavalakis[a,b], David Cocker[a,b], Thomas D. Durbin[a,b], J. Wayne Miller[a,b], Kent C. Johnson[a,b,*]

[a] University of California Riverside, College of Engineering, Center for Environmental Research and Technology (CE-CERT), Riverside, CA, 92521, United States
[b] University of California Riverside, Department of Chemical and Environmental Engineering, Riverside, CA, 92521, United States
[c] National Research Council Canada, Measurement Science and Standards, 1200 Montreal Road, Ottawa, Ontario, K1A 0R6, Canada
[d] Emissions Research and Measurement Section, Air Quality Research Division, Environment and Climate Change Canada, Ottawa, Ontario, K1A 0H3, Canada
[e] University of California Riverside, College of Engineering, Department of Mechanical Engineering, Riverside, CA, 92521, Canada
[f] Sun Set Laboratories, 10180 SW Nimbus Ave, Suite J/5, Tigard, OR, 97223, United States
[g] International Council on Clean Transportation, 1225 I Street NW, Suite 900, Washington, DC, 20005, United States
[h] Minnesota State University, Mankato College of Science, Engineering & Technology, Mankato, MN 56001, United States
[i] Now at Climate Chemistry Measurements and Research, Climate Research Division, Environment and Climate Change Canada, 4905 Dufferin St., Toronto, Ontario, M3H 5T4, Canada
[j] Now at The Department of Chemical and Biomolecular Engineering, University of Maryland, College Park, MD, 20742, United States

ARTICLE INFO

Keywords:
Black carbon
Measurement methods
Marine fuels
Loads

ABSTRACT

Knowledge of black carbon (BC) emission factors from ships is important from human health and environmental perspectives. A study of instruments measuring BC and fuels typically used in marine operation was carried out on a small marine engine. Six analytical methods measured the BC emissions in the exhaust of the marine engine operated at two load points (25% and 75%) while burning one of three fuels: a distillate marine (DMA), a low sulfur, residual marine (RMB-30) and a high-sulfur residual marine (RMG-380). The average emission factors with all instruments increased from 0.08 to 1.88 gBC/kg fuel in going from 25 to 75% load. An analysis of variance (ANOVA) tested BC emissions against instrument, load, and combined fuel properties and showed that both engine load and fuels had a statistically significant impact on BC emission factors. While BC emissions were impacted by the fuels used, none of the fuel properties investigated (sulfur content, viscosity, carbon residue and CCAI) was a primary driver for BC emissions. Of the two residual fuels, RMB-30 with the lower sulfur content, lower viscosity and lower residual carbon, had the highest BC emission factors. BC emission factors determined with the different instruments showed a good correlation with the PAS values with correlation coefficients $R2 > 0.95$. A key finding of this research is the relative BC measured values were mostly independent of load and fuel, except for some instruments in certain fuel and load combinations.

1. Introduction

Black Carbon (BC) emissions have important implications on health effects and air quality (Corbett et al., 2007; Buffaloe et al., 2014; Khan et al., 2012; Lack et al., 2008). The health effects of BC include cardiovascular and chronic lung diseases, which are linked with particulate matter (PM) (Janssen et al., 2012; Winebrake et al., 2009). BC can make up a significant component of PM. BC emissions also have climatic effects that include direct and indirect radiative forcing, influencing cloud formation, and melting of snow, glaciers, and sea ice, especially in the highly sensitive Arctic (Bond et al., 2013; Corbett et al., 2010a; Lack and Corbett, 2012). BC emitted from marine traffic in the Arctic in particular has a nearly five-times greater surface warming effect than BC emitted at mid-latitudes (Sand et al., 2013). BC is the second largest anthropogenic contributor to global warming after CO_2, due to its strong light absorbing properties (Fuglestvedt et al., 2008).

* Corresponding author. University of California Riverside, College of Engineering, Center for Environmental Research and Technology (CE-CERT), Riverside, CA, 92521, United States.
E-mail address: kjohnson@cert.ucr.edu (K.C. Johnson).

https://doi.org/10.1016/j.atmosenv.2018.03.008
Received 18 August 2017; Received in revised form 16 February 2018; Accepted 3 March 2018
Available online 09 March 2018
1352-2310/ Published by Elsevier Ltd.

Marine transportation is estimated to contribute significantly to the global BC load. Overall, shipping emissions contribute 2% of the global black carbon (BC) inventory from all sources and 8–13% of BC emissions from diesel sources (Azzara et al., 2015; Bond et al., 2013). Previous investigations reported a range of BC emission factors from ships, varying from 0.1 to 1 g/kg fuel (International Council on Combustion Engines (CIMAC), 2012; Lack et al., 2008; Corbett et al., 2010b). Having such a wide range of BC emission factors makes it challenging to evaluate the climate impacts of BC from shipping and has raised concern during international discussions of the need for BC control measures. Modeling and inventory studies have utilized a value of 0.324 g/kg fuel, with several BC inventories using 0.34 g/kg fuel (Comer et al., 2017) or 0.35 g/kg fuel (Corbett et al., 2010b; Peters et al., 2011; Winther et al., 2014). While these emission factors are within the range of reported values, they have a high degree of uncertainty. In particular, if the full uncertainty in BC emissions factors is considered, BC from ships could represent anywhere between 1.7% and 17% of global diesel source BC emissions, assuming that 2015 diesel source BC emissions are similar to those in Bond et al.'s year 2000 estimates (Bond et al., 2013; Comer et al., 2018).

One approach to improving the confidence in BC emission factors is to add to the limited data base; however, interest in real world emissions data from ships has focused on criteria pollutants and not BC. Thus, data on BC emissions from marine engines is generally limited to laboratory testing under controlled conditions (Eyring et al., 2005). Bond et al. (2013) and Petzold et al. (2013) showed that BC emissions varied depending on the measurement method used, while Lack and Corbett (2012) and references therein show that engine load and fuels used also influence BC emission factors. In this research, the focus was on the change in BC emissions with respect to these parameters: measurement method, fuels and engine load.

Marine fuel properties are known as important parameters driving PM mass and BC emission factors. For example, high sulfur, heavy fuel oil (HFO) leads to significant PM mass emissions (Wall et al., 1988; Khan et al., 2012), so environmental agencies require ships to use low sulfur fuels (LSFs) in designated emissions control areas (ECAs) in order to reduce sulfur oxides and sulfur-related PM emissions. Recently, plans were announced to further limit sulfur emissions that can arise from the use of high sulfur marine fuels (International Maritime Organization (IMO), 2017). The use of LSFs provides reductions in the sulfur-related PM emissions, however, the effect of fuel quality on BC emissions is not clear (Lack and Corbett, 2012). Some studies have suggested that switching to low sulfur heavy fuel oil (LSHFO) could reduce BC emissions due to the reduction in aromatic and long chain hydrocarbon components in the fuel, resulting in lower concentrations of BC particle nuclei (Lack et al., 2011; Lack and Corbett, 2012; Buffaloe et al., 2014). However, several authors found that LSHFO increased BC emissions, while lowering sulfur-related PM emissions (CIMAC, 2012; Aakko-Saksa et al., 2016a; Ristimäki et al., 2010; Sippula et al., 2014). In this case, the authors suggested that metal oxides in the high sulfur heavy fuel oil (HSHFO) catalyzed the oxidation of BC (Sippula et al., 2014) at lower engine loads. BC emission factors for low sulfur distillate fuels, however, are consistently lower compared with HSHFO and LSHFO (Aakko-Saksa et al., 2016a; Comer et al., 2018).

The present research study was carried out as part of a broader investigation to improve the confidence in reported BC emission factors with Phase 1 being carried out in the laboratory and Phase 2 making real world emission measurements on ocean going vessels (OGVs). Given the large range in reported BC emission values, the key objective in Phase 1 was to evaluate a number of parameters and learn whether these factors were causative for the large range of reported BC values. These factors included: fuel parameters, engine operating conditions, and BC measurement instruments. The platform for the Phase 1 research was a 2-stroke, high-speed marine engine that was operated with three different commercial marine fuels at two engine load points (25% and 75%). The three fuels included a low-sulfur content distillate marine (DMA), a low-sulfur residual marine fuel (RMB-30), and a high-sulfur residual marine fuel (RMG-380). Six different BC instruments, based on different measurement principles, were used in the research. The instruments and measurement principles included: 1) light absorption (LA), including photoacoustic spectroscopy (PAS) using a Micro Soot Sensor (MSS), filter smoke number (FSN) using an AVL 415SE-Smoke Meter, an Aethalometer and a multi-angle absorption photometer (MAAP); 2) thermal radiation using laser induced incandescence (LII); 3) thermal-optical using extra-situ and semi-continuous thermal-optical-analysis (TOA). An important outcome of this work was to understand how each instrument performed and to select a subset of instruments for real world measurements on board ships with large, 2-stroke, slow-speed diesel engines. To this end, information from this study was used to guide the planning for real-world tests on two marine vessels, the results of which will be presented in future publications.

1.1. Experimental approach

Test engine. The marine test engine was a 2-stroke, high speed, naturally aspirated, compression ignited, Detroit Diesel Model 6–71N, with a cylinder displacement of 7 L, a compression ratio of 18.7:1, a maximum speed of 1800 revolutions per minute (rpm), a maximum power of 187 kW, a brake mean effective pressure (BMEP) of 641 kPa, and a brake specific fuel consumption (BSFC) of 307 g/kWh (0.505 lb./hp-hr) at 1100 rpm. This engine was initially manufactured in the 1980s time period, and was widely used in marine applications for fishing and work boats, and as an auxiliary engine on larger vessels. Additional details on the specifications of the engine are provided in the supplementary material. The test engine was selected based on previous experience that this older, 2-stroke engine would produce carbonaceous particulate emissions with a high ratio of organic carbon to elemental carbon (OC/EC ratio) and thus produce similar particulate to that emitted from larger slow speed two stroke main engines for ocean going vessels. The engine was set up with N70, single, large spray pattern port injectors to enable it to burn a range of fuels, from distillate to the dirtiest/cheapest heavy-fuel oil (HFO). N70 injectors, with a single, large spray port, limited coking and plugging of the injection tip during testing. For testing, the engine was mounted and operated on a 600 horsepower (hp) GE DC electric engine dynamometer.

Test fuels. Three different representative commercial marine fuels with a wide range of properties were tested: a distillate marine A (DMA), a low-sulfur, residual marine B (RMB-30) and a high-sulfur, residual marine G (RMG-380). Some of the main of properties of the test fuels are provided in Table 1. This includes fuel sulfur content, density, viscosity, carbon residue, and the Calculated Carbon Aromaticity Index (CCAI). The CCAI is a measure of the ignition quality of residual fuel oil (Sarvi et al., 2008) in diesel engines and is normally a value between 800 and 880. The lower values combust better, and values > 880 are above specification. Note that the CCAI is typically a metric for residual fuels, so the value for the DMA fuel was not calculated. CCAI is calculated by:

$$CCAI = D - 140.7\log(\log(V + 0.85)) - 80.6 - 483.5\log\left(\frac{t + 273}{323}\right)$$

Table 1
Selected fuel properties.

Fuel	DMA	RMB-30	RMG-380
Sulfur wt% (ppm)	13	13.2	31,849
Density @ 15 °C (kg/L)	0.8309	0.8586	0.9826
Viscosity @ 40 °C (cSt)	2.696	–	–
Viscosity @ 50 °C (cSt)		13.73	358.9
Micro Carbon Residue (%m/m)	< 0.1	< 0.1	12.84
CCAI_calculated		769	845

Where: D = density at 15 °C (kg/m^3); V = viscosity (cST); and t = viscosity temperature (°C).

The energy content of the DMA fuel, which is similar to No.2 diesel fuel, is estimated to be 45 MJ/kg. The energy contents of the HFO fuels is estimated to be 41 MJ/kg.

The DMA is a low-sulfur distillate fuel similar to No. 2 diesel fuel that is being considered for use for marine engines operated in ECAs. The RMB-30 is a low-sulfur, heavy fuel oil (LSHFO) that is a newer fuel designed to comply with ECA fuel sulfur standards. This fuel combines the performance properties of HFO (e.g., a high flashpoint and low volatility) with a low sulfur content (EPA, 2016). The high-sulfur RMG-380 is comparable to the dirtiest and cheapest fuels often used by large ocean going vessels. Compared with the LSHFO, the RMG-380 viscosity was 100 times higher, and the sulfur level was 1000 times higher.

The residual fuels were fed from drums heated to 95 °C to ensure flow to the engine. Furthermore, the engine was run on DMA fuel at high load for 30 min prior to using the RMG-380 to ensure that the piston head temperature was above the fire point, thus serving as a glow plug when introducing the residual fuels. The test fuels are representative of commercial fuels and the broad range of properties enables an analysis of whether those properties drive BC production and also if they change the nature of the BC and co-emitted species produced such that it influences the different BC measurement technologies.

Test loads. Testing was conducted using the three fuels at 25% and 75% engine loads with the engine operating at 1100 RPM. The 25% and 75% load points were selected to provide test conditions with different OC to EC ratios. At the 25% load point, the OC/EC ratio was ~9+:1. This OC/EC ratio is similar to the 9:1 ratio that has been seen OGV main engines (Gysel et al., 2017). At the 75% load, the OC/EC ratio was ~1:1, thus allowing a measure of the instruments' response at two very different OC/EC ratios.

1.2. Measurement methods

Instruments. BC is defined as a distinct type of solid carbonaceous material, formed primarily in flames, that has a unique combination of physical properties, including strong light absorption, refractory, small and aggregated particles, and resistant to chemical reaction (Bond et al., 2013; Petzold et al., 2013). There are many analytical methods used to measure BC emissions, each relying on one or more of these properties in the detection method. To aid in the interpretation of reported data, Petzold et al. (2013) has suggested the use of terminology which makes clear what type of method has been used. For example, equivalent black carbon (eBC) for light absorption methods, refractory black carbon (rBC) for Laser Induced Incandescence, and elemental carbon (EC) for thermal-optical analysis. It is not clear if any method is considered more accurate or representative of marine BC emissions. In this study, we are investigating whether the use of a broad range of methods in past studies could have contributed to the large range of emission factors reported in the literature.

BC emissions were measured using six instruments that operate on different measurement principles associated with different properties of BC; see Table 2. The instruments in this study are widely used, thus allowing an assessment of the potential importance of measurement method on the variability of emission factors reported in the literature.

Experimental Layout. Fig. 1 provides a schematic of the experimental setup, including the four instrument sampling locations. The schematic also includes the location of a catalytic stripper and sulfur adsorbers that were used for some sample conditioning testing. In this paper, only the results for the bypass (BP) condition (i.e., without the catalytic stripper and sulfur adsorbers) are discussed. The four sampling locations represented 1:1 dilution on stack, and 1:1, 14:1, and 1400:1 dilution after the bypass and sample conditioning. Dilution was necessary for several reasons. First, it mitigates problems with heat, humidity, and lowers the PM concentration to the maximum allowed by the instrument. For example, the MAAP and Aethalometer are designed to measure particle concentrations up to 50 μg/m^3 (MAAP, 2016; Aethalometer Manual, 2016), so these instruments used a dilution of 1400:1. Another important point is that dilution also reduces the vapor pressure of the gaseous materials in the airstream such that when the exhaust is cooled, the partial vapor pressure for sulfuric acid (for example) will not exceed its saturated vapor pressure at that given temperature. This minimizes the potential for artifact condensation. Note that all sample lines were heated up to the point of dilution or the measurement instrument if no dilution was applied (red lines in Fig. 1) to reduce condensation of water, semi-volatile and volatile organics.

Different approaches were used for dilution. For the 14:1 dilution, a dilution tunnel with a partial flow dilution sampling system was used with a single venturi following the requirements of the ISO 8178-1 methods (ISO, 1996). Comparisons between FSN at 1:1 on stack and 1:1 dilution sampling points and LII instruments at the 1:1 and 14: 1 dilution sampling points showed good agreement, indicating similar results were seen for different levels of dilution. These results are presented in the Supplementary Material. The dilution air used in this process was pretreated in a unit that included silica gel to remove water, activated carbon to remove hydrocarbons, and a HEPA filter to remove PM. As per ISO-8178-1, the dilution ratio was calculated using raw and dilute concentrations of NOx and CO_2. This approach allowed the dilution ratio to be calculated by two independent methods. Comparative results met the standard of ISO 8178-1. It should be noted that the LII instrument that we initially placed in the LII #3 position did not work correctly during the testing on the DMA, so the working LII instrument that was in the LII #1 position was swapped to the #3 position for the subsequent testing on the RMG-380 and RMB-30 testing, as the 14:1 dilution point was where most of the more critical instrument comparisons were done.

The special dilution unit for the 1400:1 dilution factor used three dilutors in series. The first stage was a rotating disk dilutor (RDD, DF = 10:1), and the second was a mixing dilutor (DF = 10:1) that used a rotary vane pump to add filtered air to the RDD output. The final stage used a venturi with a 14:1 dilution ratio. These three stages provided an overall 1400:1 dilution ratio. For the diluted samples, heated lines were not needed after the dilution point because the vapor pressure of water and volatile organics were sufficiently low that condensation was negligible. In order to avoid discrepancies in particle losses between the different instruments at different locations, the residence times of the samples for each BC instrument were matched.

2. Results and discussion

BC emission factors (g/kg fuel). The BC emission factors for the six instruments, corrected for dilution, are presented in Fig. 2a and b for three fuels at the 25% and 75% loads, respectively. Results are reported as the mass of BC relative to the mass of fuel burned in g/kg units. Fuel-specific mass values are often referred to either as an 'emission index', or an 'emission factor' as used in this paper and are the primary units used in the literature to report BC emission rates. Emission factors in g/kWh are also important in other applications, so BC emission factors in these units and for NOx are also provided in the Supplementary Material.

A statistical analysis between instrument, load, and fuel factors was performed by using analysis of variance (ANOVA) methods. The results of these ANOVA analyses are presented in the *Statistical Analysis for BC Emissions for the Load, Fuel, and Instrument Factors* section of the Supplementary Material. The analyses showed that both fuels ($p = 0.000$) and engine load ($p = 0.000$) had a statistically significant impact on BC emission factors. The primary ANOVA analyses did not show statistically significant differences for the instruments, but there was a statistically significant interaction between the instrument and load factors, indicating that the differences between instruments varied a function of different loads. The results for the different loads and fuels

Table 2
Black carbon measurement instruments and associated measurement principles.

Instrument	Abbreviation	Model	Measurement Principle	Wavelength (nm)	Report Value	Detection limit (μg/m[c])	Max. Conc. (mg/m[c])
Aethalometer[a]	Aethalometer	Magee Scientific AE21	light absorption and scattering	370 and 880	eBC	0.1	0.05
Laser Induced Incandescence[b]	LII	Artium 300	thermal radiation	N/A	rBC	1	20,000
Multi-Angle Absorption Photometer[c]	MAAP	Thermo Scientific 5012	light absorption and scattering	670	eBC	0.1	0.05
Micro-Soot Sensor[d]	PAS	AVL 483	light absorption (photoacoustic)	808	eBC	1	50
TOA-Extra Situ[e]	TOA-ES	Sunset Laboratories	thermal-optical		EC	0.3–0.4 g/cm^3/ filter loading	
TOA-Semi-Continuous[f]	TOA- SC						
Smoke Meter[g]	FSN Line 1 or FSN Line 2	AVL 415SE	light absorption	420–680	eBC via FSN	20	100

[a] Aethalometer, 2016.
[b] LII, 2016.
[c] MAAP 2016.
[d] MSS, 2018.
[e] TOA-ES, 2018.
[f] TOA-SC, 2018.
[g] Smoke Meter, 2018.

are presented here, while the instrument results are discussed in greater detail in the next section.

The average emission factors over all instruments increased from 0.08 to 1.88 g/kg fuel in going from 25 to 75% load, about 24 times higher. This finding is opposite to the trend that has been reported for medium speed and large slow-speed, turbocharged, marine engines, which represent the majority of marine engines used in ocean-going service. Those engines have shown lower BC emission factors at higher loads (Agrawal et al., 2008, 2008b; Khan et al., 2012; Khan et al., 2013; Lack and Corbett, 2012; CIMAC, 2012). Lack and Corbett (2012) found that BC emission factors increased by an average factor of 3 in going from 100 to 25%, with increases of up to a factor of 6.5 for loads below 25%. This trend was attributed to the lower fuel consumption at lower loads, and to the fact that at lower loads the engine is operating outside the range where the engine is designed to operate efficiency. Higher emissions at lower load points were also seen in a CIMAC (2012) review, where BC emission factors for a medium speed engine ranged from less than 0.1 g/kg of fuel to as high as 0.8 g/kg of fuel at 10% load points. They attributed the result to the higher combustion efficiencies at the higher load points. The trend of increasing BC emission factors with increasing engine load in the present study is likely a consequence of using an older, high-speed engine where the residence time for combustion of soot is much shorter compared to medium speed and large slow-speed, turbocharged, marine engines. The test engine in this study was operating at constant speed, so and in order to triple the power output, the input fuel rate was tripled. The older engine used in this study also used a combustion cylinder design that was not improved for soot combustion and burn out as there were no PM standards at that time. While all diesel engines have excess oxygen for combustion, there are localized fuel-rich areas with insufficient air where soot is formed. Combustion design for modern engines aims for very small droplets that readily volatilize and mix with surrounding air to limit soot production and for in-cylinder swirl turbulence and time to burn out the PM. As discussed earlier, the higher speed engine and setup was selected to provide a range of PM characteristics that would be representative of those found in engines, on ocean going vessels, thus enabling a robust comparison of a number of instruments measuring BC emission factors.

In comparing the different fuels, average BC emission factors ranged from 0.13 to 0.82 g/kg fuel for the DMA, from 0.25 g/kg to 1.88 g/kg

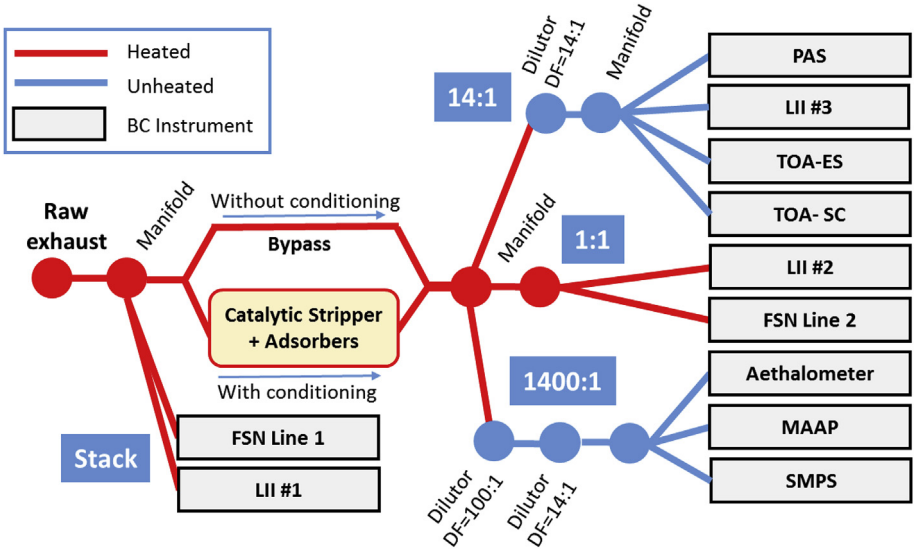

Fig. 1. Schematic of the experimental layout with dilution factor (DF) and instruments.

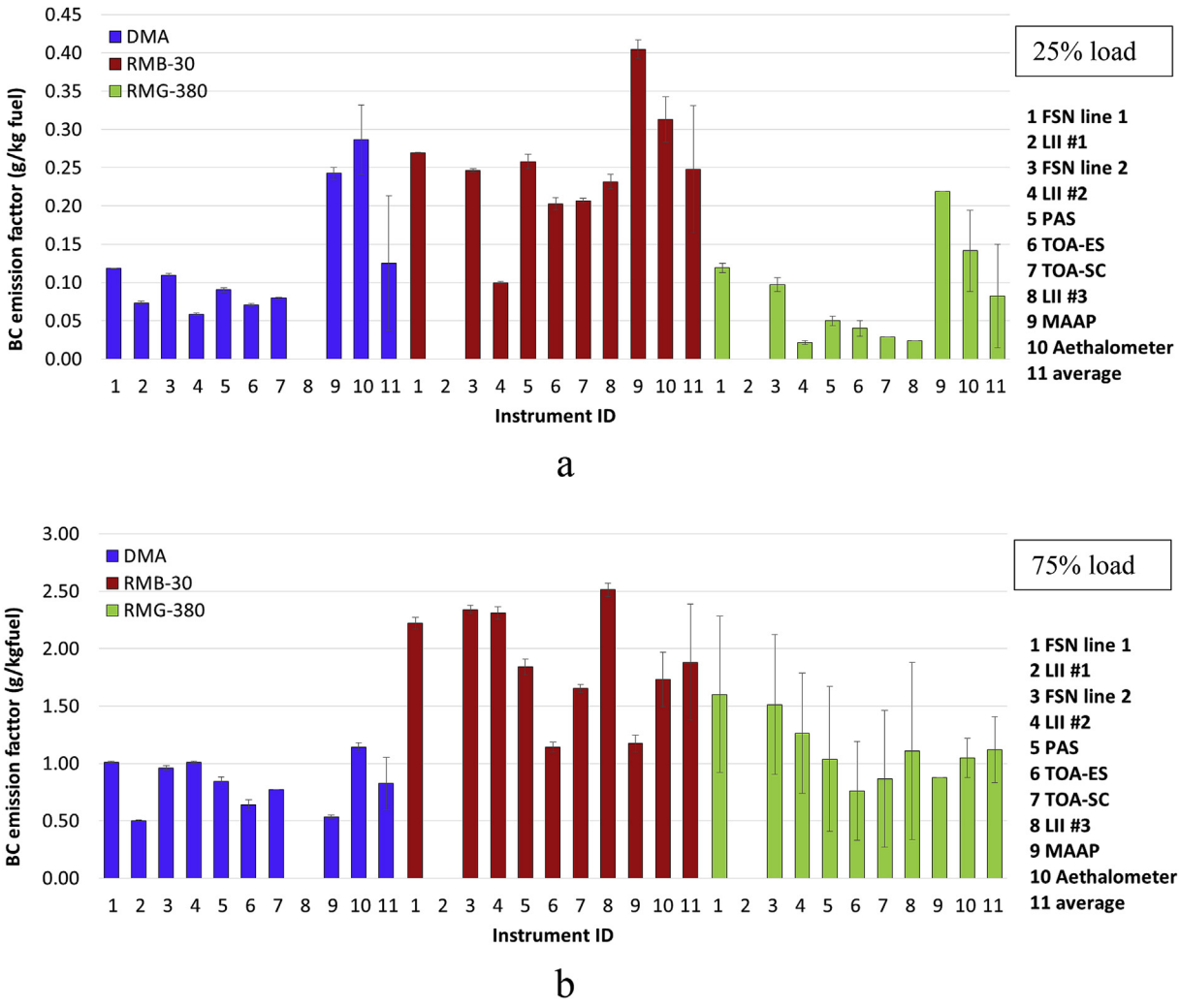

Fig. 2. a: Summary of BC Emissions Factors (g/kg fuel) at 25% Load. b: Summary of BC Emissions Factors (g/kg fuel) at 75% Load.

fuel for the RMB-30, and from 0.08 to 1.12 g/kg fuel for the RMG-380, where the lower and higher values represent the results at the 25% and 75% load points, respectively. At 25% load, the RMG-380 had the lowest emission factor but the DMA was the lowest at 75% load. The RMB-30 – the new low-sulfur HFO with a lower sulfur, viscosity and residual carbon content than the RMG-380 – showed the highest BC emission factors at both loads. The average results showed increases of about 200% in going from the RMG-380 to RMB-30 fuels at the 25% load, and increases of 97% in going from the DMA to RMB-30 fuels at the 75% load. These differences are important, but were less than the differences seen as a function of different engine loads. The difference of 35.7% between the DMA and RMG-380 fuels at the 75% load point is comparable to the average 30% difference between DMA and RMG-380 found in the literature review by Lack and Corbett (2012).

The results did not show consistent trends in BC emissions as a function of fuel sulfur levels, given that the fuel sulfur levels in the fuels varied from ~13 ppmw to 32,000 ppmw. This finding is not surprising, as BC is primarily formed from the pyrolysis of carbon moieties, and sulfur is not involved in the reaction pathways. The lack of consistent trend for BC emissions as a function of fuel sulfur has also been seen in the literature, with some studies showing higher BC emissions for lower sulfur fuels (CIMAC, 2012; Aakko-Saksa et al., 2016a; Ristimäki et al., 2010), while others have reported lower BC emissions for LSHFO fuels (Comer et al., 2018; Lack et al., 2011, Lack and Corbett, 2012; Buffaloe et al., 2014).

A second fuel factor that could be a primary driver of BC is the fuel oil viscosity, as it is a primary parameter in determining the Sauter mean droplet diameter (Nukiyama and Tanasawa, 1938; Arai et al., 1984). Since the RMG-380 was 25 times more viscous than the RMB-30, the RMG-380 should produce a larger droplet diameter in the combustion chamber and more unburned fuel in the exhaust. Again, the results showed viscosity was not a primary driver of BC emissions. A third parameter investigated was the resulting carbon residue from pyrolysis of the fuel. Here the RMG-380 with > 128 times the propensity to form char on heating as compared with RMB-30 had less BC than the RMB-30. A final parameter was the CCAI. The RMB-30 had a lower CCAI than the RMG-380, indicating that the RMB-30 had better ignition quality and that it should burn more completely. Again, there was more BC with the RMB-30 than with the RMG-380, suggesting that CCAI was not the main factor contributing to BC emissions.

One factor that could have an important impact on BC emissions is the presence of metal oxides from the porphyrins in crude oil. Some have hypothesized that the presence of metals and metal oxides in the HSHFO at lower engine loads may catalyze and enhance the oxidation of BC, which would lead to lower BC emissions for HSHFO (Sippula et al., 2014), consistent with our results. This has been seen in other studies (Sippula et al., 2014; Andreae and Gelencsér, 2006). Higher levels of inorganic material in the PM composition in biomass burning studies resulted in TOA-derived EC oxidizing at lower temperatures (Andreae and Gelencsér, 2006). In this study, refractory residuals were visually observable on the quartz filters after the NIOSH TOA-ES filter analyses for the RMG-380 samples, but were not visually observed for

the other two fuels. There was also some indication of the presence of metals in transmission electron microscope (TEM) images for the RMG-380 fuel, which will be discussed in greater detail elsewhere. The residual was likely a mix of vanadium and nickel oxides from the porphyrins in the crude (Lewan, 1984) that catalyze the oxidation of the EC. Additional analyses of the refractory residual were not available, and further investigation is needed to better understand these results.

Although the results show that fuel differences have important impacts on BC emissions, the selected fuel parameters tested in this research did not identify the key parameters or drivers for BC emissions. While this study provided important information about the relationship between fuel properties and BC emissions, future studies are needed and should investigate other fuel parameters as well as the combustion process. The results do suggest that the use of distillate fuels could provide reductions in BC emissions from marine vessels, while LSHFOs could lead to increases in BC emissions.

BC instrument comparisons. The recorded concentration of BC increased for all instruments at higher engine loads, but the increase varied among instruments. In order to get a measure of the variation in values between instruments, we constructed parity plots with the PAS instrument on the x-axis and the other instruments on the y-axis. Additional information on statistical comparisons between BC emission factors for different instruments is provided in the Supplementary Material. The PAS was selected as the basis for comparison for the BC emission factors in this section, since it was incorporated into compliance testing as part of the U.S. EPA's heavy-duty In-Use testing Measurement Allowance Project (Janssen et al., 2012) and in the aviation industry (SAE, 2011, 2013). While we have utilized the PAS as a basis of comparison for these reasons, it should be noted that this is primarily to show the range of BC emissions measurements, rather than to suggest a preference for one instrument above the others.

Values for the slope and intercept of each instrument measured relative to the PAS instrument are shown in Fig. 3. The data in Fig. 3 show three clusters of data: one at lower, medium, and higher BC readings. Values up to 4 mg/m^3 were for 25% load; values near 30 mg/m^3 were the DMA and RMG-380 data for the 75% load; and values between 60 and 80 mg/m^3 were for the RMB-30 fuel and some RMG-380 data for the 75% load. The slopes show similar trends with coefficient of determination, R^2, values > 0.95 for all instruments. The main differences between instruments are the slopes of the regressions themselves, with the slopes being > 1 for the FSN and LIIs and < 1 for the TOAs and atmospheric instruments (i.e., MAAP and Aethalometer). Additional figures showing the data at the lower concentrations in greater detail are provided in the Supplementary Material in the section *BC mass concentration presented in mass per volume units for the 25% load points*. Some additional analyses of how the slopes for each instrument change when the results for the RMB-30 and RMG-380 fuels are normalized by the DMA results are also presented in the Supplementary Material in the section *BC mass concentrations for the RMB-30 and RMG-380 Fuels Normalized by the DMA Fuels*. This additional analysis shows that most instruments continue to agree with each other as the fuel changes, with the exception of a few instruments.

The FSN and LII slopes are similar so the instruments responded similarly to BC and had a BC emission factor 1.22–1.29 times that of the PAS instrument (Fig. 3a and b). According to the manufacturer, the FSN implemented a thermophoresis loss correction in the Firmware, while the PAS does not correct for thermophoresis loss. The thermophoresis loss correction would contribute to higher readings for the FSN than PAS. The impacts of particle losses were calculated using equation (17) from Shin et al. (2008). The loss is estimated at 21%–24% for the PAS, comparable to the differences between the FSN and the PAS.

LII #2 and LII#3 sampled from the DF 1:1 location and the DF 14:1 (diluted) location, respectively. Fig. 3b shows that there is a good correlation between the PAS and LIIs, with an R^2 of 0.98 for both LIIs. The slopes of the regression for LIIs range from 1.22 to 1.30, indicating values approximately 22–30% higher than those for the PAS. Differences between the two instruments and with the PAS may be due to differences in the calibrations of the two instruments, which may have been calibrated on different particle sources. Another study also found that LIIs measured higher BC values than a PAS (Durbin et al., 2007). While the LII measurement was higher than the PAS at the 75% load point, leading to the higher regression slope, the LII measurements at the 25% load point were lower than those of the PAS, as seen in the Supplementary Material. Another study found lower readings for the LII compared to PAS at ambient level concentrations (Chan et al., 2011). The lower readings at the 25% load point could be related to the high OC content of carbonaceous particles under those conditions. If OC takes the form of a coating on the BC particles this can inhibit the particle heating such that the peak temperature suboptimal for LII detection which can bias readings. High OC content is also linked to lower maturity BC particles with different optical properties than mature BC which can also bias the measurements. In both instances, the bias is towards lower readings.

Of the two commonly used BC instruments developed for ambient air monitoring, the MAAP reported the lowest BC values. Hyvärinen et al. (2013) also found that MAAP readings underestimated BC concentrations, similar to this study, for ambient urban environments where high concentration levels of BC were found. As shown in Fig. 3c, BC values for the Aethalometer were on average 86% of those measured by the PAS method. Both ambient instruments are filter-based and known to have measurement errors introduced by light scattering off particles and filter fibers (Weingartner et al., 2003). Also the filter spot change could introduce errors up to 100%, even when corrections are applied (Lack, 2015). Some have reported scattering and filter spot change contributed to the lower readings when compared with other instruments (Petzold and Schönlinner, 2004). Another observation associated with the MAAP and Aethalometer is the relatively larger intercepts of the regressions, as shown in Fig. 3c and with more detailed plots in the Supplementary Material in the *BC mass concentration presented in mass per volume units for the 25% load points* section. The MAAP and Aethalometer sampled from the DF 1400:1 location due to their lower concentration ranges. The larger intercepts for BC at the lowest concentration levels for the high dilution could be due to slight offsets in these lower level readings for these instruments relative to the PAS that are multiplied when the exhaust concentrations are corrected for the 1400:1 dilution, as also observed by Aakko-Saksa et al. (2016a, 2016b) and IMO (2017). For the MAAP, the high organic content of the particles at low load could lead to the formation of BC-OC core shell mixtures that can contribute to a lensing effect, leading to higher measured BC concentrations (Lack et al., 2011; Leung et al., 2017; Bhandari et al., 2017). For the Aethalometer, the fact that it is calibrated based on typical atmospheric particles could lead to some of the observed differences, as it may not be properly tuned for the type of particles that were measured in this study. Because of possible errors introduced by dilution methods and the corrections needed for the light scattering off the particles and the filter, the BC instruments designed for atmospheric air measurements are not recommended for source measurements even with a significant amount of dilution.

The slope for the TOA-ES data plotted against the PAS data is 0.65, suggesting the thermal-optical method measured on average 35% lower EC values than the PAS, as shown in Fig. 3d. This finding is consistent with the results from several publications (Lack et al., 2011; Kanaya et al., 2008). One possible explanation is that PAS methods overestimate BC concentrations by detecting coatings on the BC particles (lensing effect, e.g., Knox et al., 2009, Chan et al., 2011). Comparisons can also be made between the TOA-SC and TOA-ES. Both the TOA methods are based on the NIOSH-5040 method, with the TOA-ES method operating with the normal NIOSH-5040 method, while the TOA-SC method used a modified NIOSH method that was designed to be about twice as fast as the regular protocol. As such, a main potential difference of the two instruments are the OC-EC split points. A second important difference is that the semi-continuous TOA had a vapor

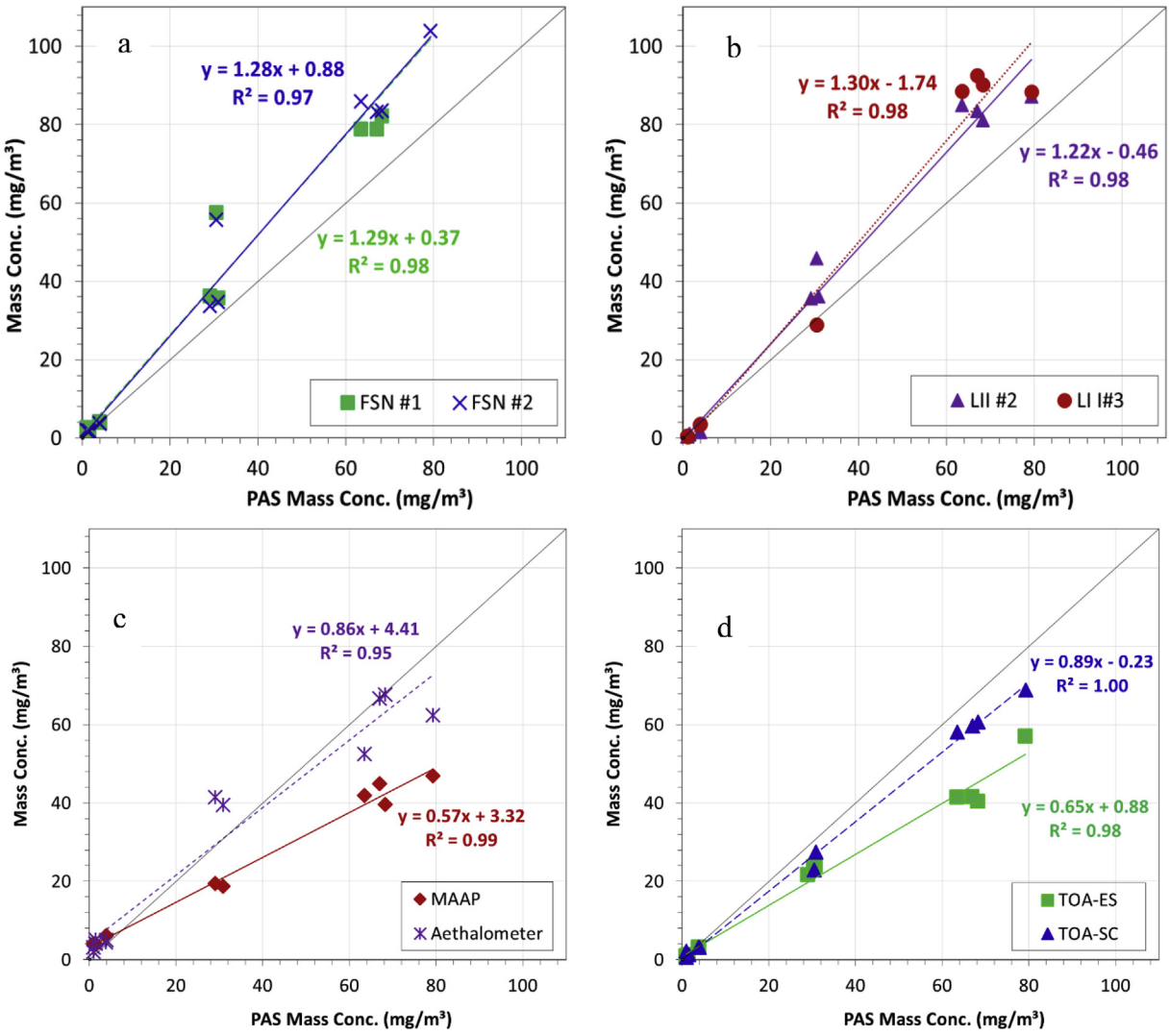

Fig. 3. Various Instrument Responses with respect to PAS Mass Concentration.

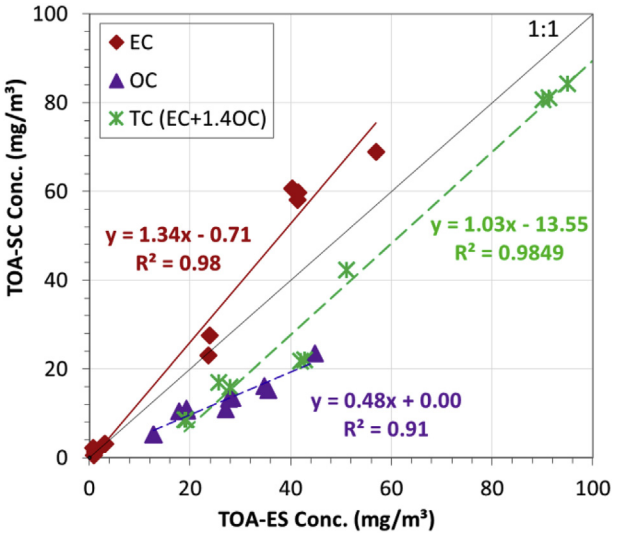

Fig. 4. Correlations between two TOA methods.

denuder installed upstream of the instrument to remove organic vapors. As shown in Fig. 4, the TOA-SC and TOA-ES showed reasonable agreement for Total Carbon (TC) emissions. The higher readings found for the TOA-ES that can probably be attributed to the TOA-SC being equipped with a vapor denuder, which removes some gas-phase organic species that might condense on the filters and contribute to OC readings. Additionally, some small organic particles may be lost via diffusion in the trap. The TOA-SC showed higher EC and lower OC readings than the TOA-ES. The opposite trends seen for the EC and OC readings coupled with the reasonable agreement in TC between the two measurement methods coincides with the instruments having different OC-EC split points, with the TOA-SC consistently having an earlier split point than the TOA-ES. The results also showed that the position of the OC-EC split point was dependent on the fuel, with the split points for the RMG 380 and DMA fuels being earlier compared to the RMB-30 fuel. This could be due to either a catalytic effect due to the presence of metal oxides or the presence of organics that are not transparent to the red laser monitoring the transmission through the filter. Deeper analysis of this fuel influence on these two TOA instruments will be presented in a subsequent paper where the catalytic stripper and sulfur adsorber results are discussed.

Particle size distributions (PSD). PSDs collected with a SMPS are shown in Fig. 5 for each of the test fuels at the 25% and 75% loads. The error bars represent the standard deviation of repeats of test runs at the different conditions. Note that due to the logarithmic scale, the error bars appear to be larger for the lower error bar than the upper error bar while they are in fact equal. A graph of PSDs on an arithmetic scale is

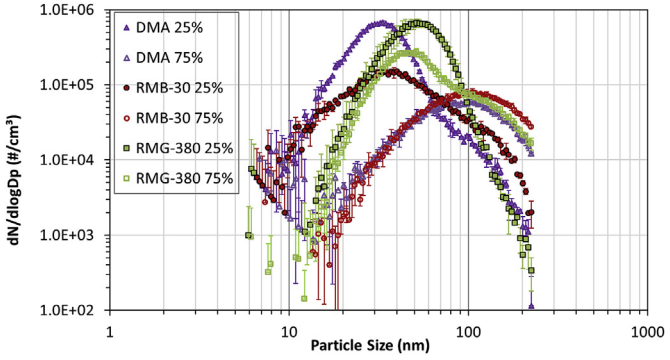

Fig. 5. Particle Size Distributions for Various Engine Loads and Fuels on a logarithmic scale.

also provided in the Supplementary Material. Generally, the PSDs at the 25% load for all three fuels had higher particle number concentrations than those at 75% loads. The PSDs for the 25% load point are comprised predominantly of small particles with peak particle diameters ranging from 30 nm to 50 nm, with higher concentrations for the DMA and RMG-380 fuels. The PSDs for the DMA and RMB-30 fuels at the 75% load points are dominated by accumulation mode particles, with peak particle diameters ranging from 90 nm to 110 nm. The PSD for the RMG-380 fuel at the 75% load point was bimodal, showing an accumulation mode peak along with a smaller peak ranging from 30 nm to 70 nm in diameter.

Bimodal PSDs for diesel engines burning HFO were observed in several studies, with peaks located in the accumulation mode (0.1–1 μm) and in the coarse mode (1–5 μm) (e.g., Linak et al., 2000). Since this SMPS measured only up to a diameter of 225 nm, only a single accumulation mode peak, with diameters ranging from 30 nm to 110 nm, could be observed in this study. These values are consistent with the peak diameters of 40 nm–100 nm previously published (Murphy et al., 2009; Linak et al., 2000; Espinoza, 2014).

The PSDs of the DMA, RMB-30, and RMG-380 at the 25% load had higher number concentrations than at the 75% load. These PSDs at the 25% load had a more pronounced nucleation mode than observed for the 75% load. The PSDs for the RMG-380 at the 75% load showed a bimodal structure and that was shifted toward bigger particles compared to the 25% load, because formation of accumulation mode particles was facilitated as the engine load went up. At the 25% load, a nucleation mode below about 25 nm can be observed, presumably predominantly nucleated by sulfuric acid particles followed by condensation of organics (Lack et al., 2009). Since the BC mass also increases with engine load, we can infer that the particles in the larger mode include BC particles.

PSD data for LSHFO is scarce in the literature, however, one study conducted by Gysel et al. (2017) measured PSDs from a crude carrier using both RMB-30 and marine gas oil (MGO) in a medium speed 4-stroke diesel engine. The results showed a peak diameter of around 30 nm–50 nm for RMB-30 and around 20 nm for the MGO, which agrees with the results at the 25% load points in this study. However, the PSDs at the 75% load for the two fuels in the current study showed larger peak diameters than in Gysel et al. (2017). The PSDs of unburned HFO should be larger than 0.5 μm, while the smaller ultrafine mode (~0.1 μm) observed in the current study may be due to more efficiently burned HFO (Linak et al., 2000).

3. Conclusions and implications

This study investigated the impacts of measurement method, fuel type, and engine load on BC emission factors from a high-speed, 2-stroke small marine engine operated at two load points with three marine fuels. Six BC analytical methods with different measurement principles were used and the BC emission factors ranged from 0.05 to 1.84 g/kg fuel based on the PAS method for three different fuels and test modes. The instruments all showed increases in BC concentrations at higher loads. At each test point measured values from the different instruments were plotted against values measured with the PAS, and the results showed a good correlation with R^2 values > 0.95. The slope of the regression plots against the PAS values ranged from 0.57 to 1.30, with the slopes being > 1 for the FSN and LIIs and < 1 for the TOAs and ambient instruments (i.e., MAAP and Aethalometer). The response of the instruments relative to each other was similar after changing fuels, except for a few instruments. This work also provided important information on instrument performance that was subsequently used to plan real-world tests of two OGVs with large, 2-stroke, slow-speed diesel engines, that will be presented elsewhere.

A key finding in this research is that the variations in BC measurement methods, cannot account for the ten-fold range of BC emission factors reported in the literature. As such, other factors, such as engine load, selected fuel properties, and engine characteristics, likely contribute to the large variations in BC emission factors. Load, in particular, had an important impact for this older, small, high-speed engine, with increases greater than a factor of 10 in BC emission factors seen in going from 25% to 75% loads. The observation of large differences in BC emission factors as a function of load has also been seen in a wider range of studies in the literature, albeit showing trends of higher emissions at lower loads, opposite to the trends seen for the particular engine in this study.

While this study provided important information about the relationship between fuel properties and BC emissions, future studies are needed and should investigate other fuel parameters as well as the combustion processes associated with engines more typically used in modern ocean going vessels. The results do suggest that the use of distillate fuels reduces BC emissions from marine vessels, as distillate fuels generally had lower black carbon emissions. The conventional HFO showed higher emissions than the DMA fuel at the 75% load, similar to the results found in the Lack and Corbett (2012) review of a wider range of studies, but not at the lower 25% load point. The new, low-sulfur residual fuel had the highest BC emissions factor of the three fuels tested, which raises questions as to what the BC emission factors will be when an intermediate fuel oil is made by blending this stream to control sulfur levels. More data need to be collected to ensure that the lower sulfur limits set for fuels lower both sulfur oxides and PM levels as intended in the IMO regulation. Interestingly, the trends in BC emissions did not show consistent trends as a function of some of the most important fuel properties, including sulfur content, viscosity, carbon residue, or the Calculated Carbon Aromaticity Index, so more research is needed to ferret out the primary parameters driving BC production.

The differences in BC emissions as a function of load and fuel type suggest that attention must be given to these parameters in developing test protocols for measuring BC emissions on ocean going vessels. It also suggests that models of marine BC emissions need to incorporate a broader range of BC emissions factors to account for the range of fuels and loads found in typical in-use operation of marine vessels.

Acknowledgements

The authors thank the following organizations and individuals for their valuable contributions to this project.

We acknowledge funding from the International Council on Clean Transportation. Yue Lin was funded by NSF grant #1233038.

We acknowledge the participation of Dr. Gavin McMeeking from Handix Scientific, LLC, and Dr. John Koupal from Eastern Research Group in this program. We acknowledge Dr. Roya Bahreini, Mr. Don Pacocha, Mr. Eddie O'Neal, Mr. Mark Villela, Dr. Lindsay Hatch, Mr. Justin Hernandez Dingle, Mr. Daniel Gomez and Ms. Lauren Aycock of the University of California, Riverside and Mr. David Buote from

Environment and Climate Change Canada for their contributions in conducting the emissions testing for this program.

We acknowledge AVL for providing the Smoke Meter, the South Coast Air Quality Management District for providing the Aethalometer, and the California Air Resources Board for providing the EEPS.

Appendix A. Supplementary data

Supplementary data related to this article can be found at http://dx.doi.org/10.1016/j.atmosenv.2018.03.008.

References

Aakko-Saksa, P., Murtonen, T., Vesala, H., Koponen, P., Nyyssönen, S., Puustinen, H., Lehtoranta, K., Timonen, H., Teinilä, K., Hillamo, R., Karjalainen, P., Kuittinen, N., Simonen, P., Rönkkö, T., Keskinen, J., Saukko, E., Tutuianu, M., Fischerleitner, R., Pirjola, L., Brunila, O., Hämäläinen, E., 2016a. Black carbon measurements using different marine fuels. In: Conference Paper at the 28th CIMAC World Congress on Combustion Engines, CIMAC Congress, Helsinki, Finland, Paper No. 68.

Aakko-Saksa, P., Murtonen, T., Vesala, H., Koponen, P., Nyyssönen, S., Puustinen, H., Lehtoranta, K., Timonen, H., Teinilä, K., Hillamo, R., Karjalainen, P., Kuittinen, N., Simonen, P., Rönkkö, T., Keskinen, J., Saukko, E., Tutuianu, M., Fischerleitner, R., Pirjola, L., Brunila, O., Hämäläinen, E., 2016b. Sea-Effects BC Black carbon measurements from ship engine when using different marine fuels. In: Presented at the ICCT's 3rd and Final Workshop on Marine Black Carbon Emissions: BC Control Strategies, (Vancouver, Canada, September).

Aethalometer Manual Website, 2016. http://www.mageesci.com/images/stories/docs/Aethalometer_book_2005.07.03.pdf. (access 16.09.10).

Agrawal, H., Malloy, Q.G., Welch, W.A., Miller, J.W., Cocker, D.R., 2008. In-use gaseous and particulate matter emissions from a modern ocean going container vessel. Atmos. Environ. 42, 5504–5510.

Agrawal, H., Welch, W.A., Miller, J.W., Cocker, D.R., 2008b. Emission measurements from a crude oil tanker at sea. Environ. Sci. Technol. 42 (19), 7098–7103.

Andreae, M.O., Gelencsér, A., 2006. Black carbon or brown carbon? The nature of light-absorbing carbonaceous aerosols. Atmos. Chem. Phys. 6, 3131–3148.

Arai, M., Tabata, M., Hiroyasu, H., Shimizu, M., 1984. Disintegrating Process and Spray Characterization of Fuel Jet Injected by a Diesel Nozzle. (SAE Technical Paper).

Azzara, A., Minjares, R., Rutherford, D., 2015. Needs and opportunities to reduce black carbon emissions from maritime shipping. Assessment 118, 5380–5552.

Bhandari, J., China, S., Onasch, T., Wolff, L., Lambe, A., Davidovits, P., Cross, E., Ahern, A., Olfert, J., Dubey, M., Mazzoleni, C., 2017. Effect of thermodenuding on the structure of nascent flame soot aggregates. Atmosphere 8 (9), 166.

Bond, T.C., Doherty, S.J., Fahey, D.W., Forster, P.M., Berntsen, T., DeAngelo, B.J., Flanner, M.G., Ghan, S., Kärcher, B., Koch, D., Kinne, S., 2013. Bounding the role of black carbon in the climate system: a scientific assessment. J. Geophys. Res. 118, 5380–5552.

Buffaloe, G.M., Lack, D.A., Williams, E.J., Coffman, D., Hayden, K.L., Lerner, B.M., Li, S.M., Nuaaman, I., Massoli, P., Onasch, T.B., Quinn, P.K., 2014. Black carbon emissions from in-use ships: a California regional assessment. Atmos. Chem. Phys. 14, 1881–1896.

Chan, T.W., Brook, J.R., Smallwood, G.J., Lu, G., 2011. Time-resolved measurements of black carbon light absorption enhancement in urban and near-urban locations of southern Ontario, Canada. Atmos. Chem. Phys. 11, 10407–10432.

CIMAC - International Council on Combustion Engines, 2012. Background information on black carbon emissions from large marine and stationary diesel engines-definition, measurement methods, emission factors and abatement technologies, Main, Germany. http://www.cimac.com/cms/upload/workinggroups/WG5/black_carbon.pdf, Accessed date: 16 December 2015.

Comer, B., Olmer, N., Mao, X., Roy, B., Rutherford, D., 2017. Prevalence of Heavy Fuel Oil and Black Carbon in Arctic Shipping, 2015 to 2025. The International Council on Clean Transportation (ICCT), Washington, DC. http://www.theicct.org/sites/default/files/publications/HFO-Arctic_ICCT_Report_01052017_vF.pdf, Accessed date: 17 June 2015.

Comer, B., Olmer, N.S., Mao, X., Roy, B., Rutherford, D., 2017. Black Carbon Emissions and Fuel Use in Global Shipping. ICCT, Washington, DC.

Corbett, J.J., Winebrake, J.J., Green, E.H., Kasibhatla, P., Eyring, V., Lauer, A., 2007. Mortality from ship emissions: a global assessment. Environ. Sci. Technol. 41, 8512–8518.

Corbett, J.J., Winebrake, J.J., Green, E.H., 2010a. An assessment of technologies for reducing regional short-lived climate forcers emitted by ships with implications for Arctic shipping. Carbon Manag. 1, 207–225.

Corbett, J.J., Lack, D.A., Winebrake, J.J., Harder, S., Silberman, J.A., Gold, M., 2010b. Arctic shipping emissions inventories and future scenarios. Atmos. Chem. Phys. 10, 9689–9704.

Durbin, T.D., Johnson, K., Cocker, D.R., Miller, J.W., Maldonado, H., Shah, A., Ensfield, C., Weaver, C., Akard, M., Harvey, N., Symon, J., 2007. Evaluation and comparison of portable emissions measurement systems and federal reference methods for emissions from a back-up generator and a diesel truck operated on a chassis dynamometer. Environ. Sci. Technol. 41, 6199–6204.

U.S. Environmental Protection Agency (EPA) Website, 2016. https://nepis.epa.gov/Exe/ZyPDF.cgi/P100EG0X.PDF?Dockey=P100EG0X.PDF. (access 16.07.10).

Espinoza, C., 2014. Particle Emissions from Vehicles (SI-PFI and SI-DI) at High Speed and from Large Ocean-going Vessels. Masters Thesis. University of California at Riverside, College of Engineering, Department of Chemical and Environmental Engineering (December).

Eyring, V., Köhler, H.W., Van Aardenne, J., Lauer, A., 2005. Emissions from international shipping: 1. The last 50 years. J. Geophys. Res. 110 D17305.

Fuglestvedt, J., Berntsen, T., Myhre, G., Rypdal, K., Skeie, R.B., 2008. Climate forcing from the transport sectors. Proc. Natl. Acad. Sci. U. S. A 105, 454–458.

Gysel, N.R., Welch, W.A., Johnson, K., Miller, W., Cocker III, D.R., 2017. Detailed analysis of criteria and particle emissions from a very large crude Carrier using a novel ECA fuel. Environ. Sci. Technol. 51, 1868–1875.

Hyvärinen, A.P., Vakkari, V., Laakso, L., Hooda, R.K., Sharma, V.P., Panwar, T.S., Beukes, J.P., Van Zyl, P.G., Josipovic, M., Garland, R.M., Andreae, M.O., 2013. Correction for a measurement artifact of the Multi-Angle Absorption Photometer (MAAP) at high black carbon mass concentration levels. Atmos. Meas. Tech 6, 81–90.

International Maritime Organization (IMO) Website, 2017. http://www.imo.org/en/OurWork/environment/pollutionprevention/airpollution/pages/sulphur-oxides-(sox)--regulation-14.aspx. (access 17.05.10).

International Organization for Standardization (ISO), 1996. ISO8178–2, Reciprocating Internal Combustion Engines: Exhaust Emission Measurement. Part-2: Measurement of Gaseous Particulate Exhaust Emissions at Site. ISO, Geneva, Switzerland.

Janssen, N.A., Hoek, G., Simic-Lawson, M., Fischer, P., Van Bree, L., Ten Brink, H., Keuken, M., Atkinson, R.W., Anderson, H.R., Brunekreef, B., Cassee, F.R., 2012. Black carbon as an additional indicator of the adverse health effects of airborne particles compared with PM_{10} $PM_{2.5}$. Environ. Health Perspect. 119, 1691–1699.

Kanaya, Y., Komazaki, Y., Pochanart, P., Liu, Y., Akimoto, H., Gao, J., Wang, T., Wang, Z., 2008. Mass concentrations of black carbon measured by four instruments in the middle of Central East China in June 2006. Atmos. Chem. Phys. 8, 7637–7649.

Khan, M.Y., Giordano, M., Gutierrez, J., Welch, W.A., Asa-Awuku, A., Miller, J.W., Cocker III, D.R., 2012. Benefits of two mitigation strategies for container vessels: cleaner engines and cleaner fuels. Environ. Sci. Technol. 46, 5049–5056.

Khan, M.Y., Ranganathan, S., Agrawal, H., Welch, W.A., Laroo, C., Miller, J.W., Cocker III, D.R., 2013. Measuring in-use ship emissions with international and US federal methods. J. Air Waste Manag. Assoc. 63 (3), 284–291.

Knox, A., Evans, G.J., Brook, J.R., Yao, X., Jeong, C.H., Godri, K.J., Sabaliauskas, K., Slowik, J.G., 2009. Mass absorption cross-section of ambient black carbon aerosol in relation to chemical age. Aerosol. Sci. Technol. 43, 522–532.

Lack, D., 2015. BC measurement overview, and considerations for a community approach to measurement. In: Presented at the 2nd Workshop on Marine Black Carbon Emissions, (Utrecht, Netherlands, September).

Lack, D.A., Corbett, J.J., 2012. Black carbon from ships: a review of the effects of ship speed, fuel quality and exhaust gas scrubbing. Atmos. Chem. Phys. 12, 3985–4000.

Lack, D., Lerner, B., Granier, C., Baynard, T., Lovejoy, E., Massoli, P., Ravishankara, A.R., Williams, E., 2008. Light absorbing carbon emissions from commercial shipping. Geophys. Res. Lett. 35 L13815.

Lack, D.A., Cappa, C.D., Langridge, J., Bahreini, R., Buffaloe, G., Brock, C., Cerully, K., Coffman, D., Hayden, K., Holloway, J., Lerner, B., 2011. Impact of fuel quality regulation and speed reductions on shipping emissions: implications for climate and air quality. Environ. Sci. Technol. 45, 9052–9060.

Lack, D.A., Corbett, J.J., Onasch, T., Lerner, B., Massoli, P., Quinn, P.K., Bates, T.S., Covert, D.S., Coffman, D., Sierau, B., Herndon, S., 2009. Particulate emissions from commercial shipping: Chemical, physical, and optical properties. J. Geophys. Res. Atmos. 114 (D7).

Lewan, M.D., 1984. Factors controlling the proportionality of vanadium to nickel in crude oils. Geochem. Cosmochim. Acta 48, 2231–2238.

LII 300 Brochure Website, 2016. http://www.artium.com/wp-content/uploads/2017/01/II300_Brochure_Updates_v4.pdf. (access 16.09.10).

Linak, W.P., Miller, C.A., Wendt, J.O., 2000. Comparison of particle size distributions and elemental partitioning from the combustion of pulverized coal and residual fuel oil. J. Air Waste Manag. Assoc. 50, 1532–1544.

Leung, K.K., Schnitzler, E.G., Dastanpour, R., Rogak, S.N., Jäger, W., Olfert, J.S., 2017. Relationship between coating-induced soot aggregate restructuring and primary particle number. Environ. Sci. Technol. 51 (15), 8376–8383.

Multi Angle Absorption Photometer (MAAP) Instruction Manual 5012 Website, 2016. https://tools.thermofisher.com/content/sfs/manuals/EPM-manual-Model%205012%20MAAP.pdf. (access 16.09.10).

MSS 483 Website, 2018. https://www.avl.com/-/mssplus-avl-micro-soot-sensor. (access 18.02.10).

Murphy, S.M., Agrawal, H., Sorooshian, A., Padró, L.T., Gates, H., Hersey, S., Welch, W.A., Jung, H., Miller, J.W., Cocker III, D.R., Nenes, A., 2009. Comprehensive simultaneous shipboard and airborne characterization of exhaust from a modern container ship at sea. Environ. Sci. Technol. 43, 4626–4640.

Nukiyama, S., Tanasawa, Y., 1938. An experiment on the atomization of liquid by means of an air stream (1. Report). Trans. Jpn. Soc. Mech. Eng. 4 (14), 128–135. –. https://doi.org/10.1299/kikai1938.4.128.

Peters, G.P., Nilssen, T.B., Lindholt, L., Eide, M.S., Glomsrod, S., Eide, L.I., Fuglestvedt, J.S., 2011. Future emissions from shipping and petroleum activities in the Arctic. Atmos. Chem. Phys. 11, 5305–5320.

Petzold, A., Schönlinner, M., 2004. Multi-angle absorption photometry—a new method for the measurement of aerosol light absorption and atmospheric black carbon. J. Aerosol Sci. 35, 421–441.

Petzold, A., Ogren, J.A., Fiebig, M., Laj, P., Li, S.M., Baltensperger, U., Holzer-Popp, T., Kinne, S., Pappalardo, G., Sugimoto, N., Wehrli, C., 2013. Recommendations for reporting" black carbon" measurements. Atmos. Chem. Phys. 13, 8365–8379.

Ristimäki, J., Hellen, G., Lappi, M., 2010. Chemical and Physical Characterization of Exhaust Particulate Matter from a Marine Medium Speed Diesel Engine. In: Presented at the International Council on Combustion Engines, CIMAC Congress, Bergen, Paper

No. 73.
SAE Aerospace Recommended Practice 1179 Rev D, 2011. Aircraft Gas Turbine Engine Exhaust Smoke Measurement. SAE International, Warrendale, PA, USA. https://saemobilus.sae.org/content/arp1179.
SAE Aerospace Information Report 6241, 2013. Procedure for the Continuous Sampling and Measurement of Non-volatile Particle Emissions from Aircraft Turbine Engines. SAE International, Warrendale, PA, USA. https://saemobilus.sae.org/content/air6241.
Sand, M., Berntsen, T.K., Seland, Ø., Kristjánsson, J.E., 2013. Arctic surface temperature change to emissions of black carbon within Arctic or midlatitudes. J. Geophys. Res. Atmos. 118, 7788–7798.
Sarvi, A., Fogelholm, C.J., Zevenhoven, R., 2008. Emissions from large-scale medium-speed diesel engines: 2. Influence of fuel type and operating mode. Fuel Process. Technol. 89 (5), 520–527.
Shin, W.G., Mulholland, G.W., Kim, S.C., Pui, D.Y.H., 2008. Experimental study of filtration efficiency of nanoparticles below 20 nm at elevated temperatures. J. Aerosol Sci. 39, 488–499.
Sippula, O., Stengel, B., Sklorz, M., Streibel, T., Rabe, R., Orasche, J., Lintelmann, J., Michalke, B., Abbaszade, G., Radischat, C., Groger, T., 2014. Particle emissions from a marine engine: chemical composition and aromatic emission profiles under various operating conditions. Environ. Sci. Technol. 48, 11721–11729.
Smoke Meter Website, 2018, https://www.avl.com/-/avl-smoke-meter (access 18.02.10).
TOA-ES website, 2018. http://www.sunlab.com/lab-oc-ec-aerosol-analyzer/. (access 18.02.10).
TOA-SC website, 2018. http://www.sunlab.com/model-4-semi-continuous-oc-ec-field-analyzer/. (access 18.02.10).
Wall, J.C., Shimpi, S.A., Yu, M.L., 1988. Fuel Sulfur Reduction for Control of Diesel Particulate Emissions. http://dx.doi.org/10.4271/2006-11-872139. SAE Tech. Pap. No. 872139.
Weingartner, E., Saathoff, H., Schnaiter, M., Streit, N., Bitnar, B., Baltensperger, U., 2003. Absorption of light by soot particles: determination of the absorption coefficient by means of aethalometers. J. Aerosol Sci. 34, 1445–1463.
Winebrake, J.J., Corbett, J.J., Green, E.H., Lauer, A., Eyring, V., 2009. Mitigating the health impacts of pollution from oceangoing shipping: an assessment of low-sulfur fuel mandates. Environ. Sci. Technol. 43, 4776–4782.
Winther, M., Christensen, J.H., Plejdrup, M.S., Ravn, E.S., Ericsson, O.F., Kristensen, H.O., 2014. Emission inventories for ships in the Arctic based on satellite sampled AIS data. Atmos. Environ. 91, 1–14.